

# Search for $D^0$ - $\bar{D}^0$ mixing in $D^0 \rightarrow K^+ \pi^-$ decays and measurement of the doubly-Cabibbo-suppressed decay rate

K. Abe,<sup>10</sup> K. Abe,<sup>46</sup> N. Abe,<sup>49</sup> I. Adachi,<sup>10</sup> H. Aihara,<sup>48</sup> M. Akatsu,<sup>24</sup> Y. Asano,<sup>53</sup>  
 T. Aso,<sup>52</sup> V. Aulchenko,<sup>2</sup> T. Aushev,<sup>14</sup> T. Aziz,<sup>44</sup> S. Bahinipati,<sup>6</sup> A. M. Bakich,<sup>43</sup>  
 Y. Ban,<sup>36</sup> M. Barbero,<sup>9</sup> A. Bay,<sup>20</sup> I. Bedny,<sup>2</sup> U. Bitenc,<sup>15</sup> I. Bizjak,<sup>15</sup> S. Blyth,<sup>29</sup>  
 A. Bondar,<sup>2</sup> A. Bozek,<sup>30</sup> M. Bračko,<sup>22,15</sup> J. Brodzicka,<sup>30</sup> T. E. Browder,<sup>9</sup> M.-C. Chang,<sup>29</sup>  
 P. Chang,<sup>29</sup> Y. Chao,<sup>29</sup> A. Chen,<sup>26</sup> K.-F. Chen,<sup>29</sup> W. T. Chen,<sup>26</sup> B. G. Cheon,<sup>4</sup>  
 R. Chistov,<sup>14</sup> S.-K. Choi,<sup>8</sup> Y. Choi,<sup>42</sup> Y. K. Choi,<sup>42</sup> A. Chuvikov,<sup>37</sup> S. Cole,<sup>43</sup>  
 M. Danilov,<sup>14</sup> M. Dash,<sup>55</sup> L. Y. Dong,<sup>12</sup> R. Dowd,<sup>23</sup> J. Dragic,<sup>23</sup> A. Drutskoy,<sup>6</sup>  
 S. Eidelman,<sup>2</sup> Y. Enari,<sup>24</sup> D. Epifanov,<sup>2</sup> C. W. Everton,<sup>23</sup> F. Fang,<sup>9</sup> S. Fratina,<sup>15</sup>  
 H. Fujii,<sup>10</sup> N. Gabyshev,<sup>2</sup> A. Garmash,<sup>37</sup> T. Gershon,<sup>10</sup> A. Go,<sup>26</sup> G. Gokhroo,<sup>44</sup>  
 B. Golob,<sup>21,15</sup> M. Grosse Perdekamp,<sup>38</sup> H. Guler,<sup>9</sup> J. Haba,<sup>10</sup> F. Handa,<sup>47</sup> K. Hara,<sup>10</sup>  
 T. Hara,<sup>34</sup> N. C. Hastings,<sup>10</sup> K. Hasuko,<sup>38</sup> K. Hayasaka,<sup>24</sup> H. Hayashii,<sup>25</sup> M. Hazumi,<sup>10</sup>  
 E. M. Heenan,<sup>23</sup> I. Higuchi,<sup>47</sup> T. Higuchi,<sup>10</sup> L. Hinz,<sup>20</sup> T. Hojo,<sup>34</sup> T. Hokuue,<sup>24</sup>  
 Y. Hoshi,<sup>46</sup> K. Hoshina,<sup>51</sup> S. Hou,<sup>26</sup> W.-S. Hou,<sup>29</sup> Y. B. Hsiung,<sup>29</sup> H.-C. Huang,<sup>29</sup>  
 T. Igaki,<sup>24</sup> Y. Igarashi,<sup>10</sup> T. Iijima,<sup>24</sup> A. Imoto,<sup>25</sup> K. Inami,<sup>24</sup> A. Ishikawa,<sup>10</sup> H. Ishino,<sup>49</sup>  
 K. Itoh,<sup>48</sup> R. Itoh,<sup>10</sup> M. Iwamoto,<sup>3</sup> M. Iwasaki,<sup>48</sup> Y. Iwasaki,<sup>10</sup> R. Kagan,<sup>14</sup> H. Kakuno,<sup>48</sup>  
 J. H. Kang,<sup>56</sup> J. S. Kang,<sup>17</sup> P. Kapusta,<sup>30</sup> S. U. Kataoka,<sup>25</sup> N. Katayama,<sup>10</sup> H. Kawai,<sup>3</sup>  
 H. Kawai,<sup>48</sup> Y. Kawakami,<sup>24</sup> N. Kawamura,<sup>1</sup> T. Kawasaki,<sup>32</sup> N. Kent,<sup>9</sup> H. R. Khan,<sup>49</sup>  
 A. Kibayashi,<sup>49</sup> H. Kichimi,<sup>10</sup> H. J. Kim,<sup>19</sup> H. O. Kim,<sup>42</sup> Hyunwoo Kim,<sup>17</sup> J. H. Kim,<sup>42</sup>  
 S. K. Kim,<sup>41</sup> T. H. Kim,<sup>56</sup> K. Kinoshita,<sup>6</sup> P. Koppenburg,<sup>10</sup> S. Korpar,<sup>22,15</sup> P. Križan,<sup>21,15</sup>  
 P. Krokovny,<sup>2</sup> R. Kulasiri,<sup>6</sup> C. C. Kuo,<sup>26</sup> H. Kurashiro,<sup>49</sup> E. Kurihara,<sup>3</sup> A. Kusaka,<sup>48</sup>  
 A. Kuzmin,<sup>2</sup> Y.-J. Kwon,<sup>56</sup> J. S. Lange,<sup>7</sup> G. Leder,<sup>13</sup> S. E. Lee,<sup>41</sup> S. H. Lee,<sup>41</sup>  
 Y.-J. Lee,<sup>29</sup> T. Lesiak,<sup>30</sup> J. Li,<sup>40</sup> A. Limosani,<sup>23</sup> S.-W. Lin,<sup>29</sup> D. Liventsev,<sup>14</sup>  
 J. MacNaughton,<sup>13</sup> G. Majumder,<sup>44</sup> F. Mandl,<sup>13</sup> D. Marlow,<sup>37</sup> T. Matsuishi,<sup>24</sup>  
 H. Matsumoto,<sup>32</sup> S. Matsumoto,<sup>5</sup> T. Matsumoto,<sup>50</sup> A. Matyja,<sup>30</sup> Y. Mikami,<sup>47</sup>  
 W. Mitaroff,<sup>13</sup> K. Miyabayashi,<sup>25</sup> Y. Miyabayashi,<sup>24</sup> H. Miyake,<sup>34</sup> H. Miyata,<sup>32</sup> R. Mizuk,<sup>14</sup>  
 D. Mohapatra,<sup>55</sup> G. R. Moloney,<sup>23</sup> G. F. Moorhead,<sup>23</sup> T. Mori,<sup>49</sup> A. Murakami,<sup>39</sup>  
 T. Nagamine,<sup>47</sup> Y. Nagasaka,<sup>11</sup> T. Nakadaira,<sup>48</sup> I. Nakamura,<sup>10</sup> E. Nakano,<sup>33</sup> M. Nakao,<sup>10</sup>  
 H. Nakazawa,<sup>10</sup> Z. Natkaniec,<sup>30</sup> K. Neichi,<sup>46</sup> S. Nishida,<sup>10</sup> O. Nitoh,<sup>51</sup> S. Noguchi,<sup>25</sup>  
 T. Nozaki,<sup>10</sup> A. Ogawa,<sup>38</sup> S. Ogawa,<sup>45</sup> T. Ohshima,<sup>24</sup> T. Okabe,<sup>24</sup> S. Okuno,<sup>16</sup>  
 S. L. Olsen,<sup>9</sup> Y. Onuki,<sup>32</sup> W. Ostrowicz,<sup>30</sup> H. Ozaki,<sup>10</sup> P. Pakhlov,<sup>14</sup> H. Palka,<sup>30</sup>  
 C. W. Park,<sup>42</sup> H. Park,<sup>19</sup> K. S. Park,<sup>42</sup> N. Parslow,<sup>43</sup> L. S. Peak,<sup>43</sup> M. Pernicka,<sup>13</sup>  
 J.-P. Perroud,<sup>20</sup> M. Peters,<sup>9</sup> L. E. Piilonen,<sup>55</sup> A. Poluektov,<sup>2</sup> F. J. Ronga,<sup>10</sup> N. Root,<sup>2</sup>  
 M. Rozanska,<sup>30</sup> H. Sagawa,<sup>10</sup> M. Saigo,<sup>47</sup> S. Saitoh,<sup>10</sup> Y. Sakai,<sup>10</sup> H. Sakamoto,<sup>18</sup>  
 T. R. Sarangi,<sup>10</sup> M. Satapathy,<sup>54</sup> N. Sato,<sup>24</sup> O. Schneider,<sup>20</sup> J. Schümann,<sup>29</sup> C. Schwanda,<sup>13</sup>  
 A. J. Schwartz,<sup>6</sup> T. Seki,<sup>50</sup> S. Semenov,<sup>14</sup> K. Senyo,<sup>24</sup> Y. Settai,<sup>5</sup> R. Seuster,<sup>9</sup>  
 M. E. Sevior,<sup>23</sup> T. Shibata,<sup>32</sup> H. Shibuya,<sup>45</sup> B. Shwartz,<sup>2</sup> V. Sidorov,<sup>2</sup> V. Siegle,<sup>38</sup>  
 J. B. Singh,<sup>35</sup> A. Somov,<sup>6</sup> N. Soni,<sup>35</sup> R. Stamen,<sup>10</sup> S. Stanić,<sup>53,\*</sup> M. Starić,<sup>15</sup> A. Sugi,<sup>24</sup>  
 A. Sugiyama,<sup>39</sup> K. Sumisawa,<sup>34</sup> T. Sumiyoshi,<sup>50</sup> S. Suzuki,<sup>39</sup> S. Y. Suzuki,<sup>10</sup> O. Tajima,<sup>10</sup>  
 F. Takasaki,<sup>10</sup> K. Tamai,<sup>10</sup> N. Tamura,<sup>32</sup> K. Tanabe,<sup>48</sup> M. Tanaka,<sup>10</sup> G. N. Taylor,<sup>23</sup>

Y. Teramoto,<sup>33</sup> X. C. Tian,<sup>36</sup> S. Tokuda,<sup>24</sup> S. N. Tovey,<sup>23</sup> K. Trabelsi,<sup>9</sup> T. Tsuboyama,<sup>10</sup> T. Tsukamoto,<sup>10</sup> K. Uchida,<sup>9</sup> S. Uehara,<sup>10</sup> T. Uglov,<sup>14</sup> K. Ueno,<sup>29</sup> Y. Unno,<sup>3</sup> S. Uno,<sup>10</sup> Y. Ushiroda,<sup>10</sup> G. Varner,<sup>9</sup> K. E. Varvell,<sup>43</sup> S. Villa,<sup>20</sup> C. C. Wang,<sup>29</sup> C. H. Wang,<sup>28</sup> J. G. Wang,<sup>55</sup> M.-Z. Wang,<sup>29</sup> M. Watanabe,<sup>32</sup> Y. Watanabe,<sup>49</sup> L. Widhalm,<sup>13</sup> Q. L. Xie,<sup>12</sup> B. D. Yabsley,<sup>55</sup> A. Yamaguchi,<sup>47</sup> H. Yamamoto,<sup>47</sup> S. Yamamoto,<sup>50</sup> T. Yamanaka,<sup>34</sup> Y. Yamashita,<sup>31</sup> M. Yamauchi,<sup>10</sup> Heyoung Yang,<sup>41</sup> P. Yeh,<sup>29</sup> J. Ying,<sup>36</sup> K. Yoshida,<sup>24</sup> Y. Yuan,<sup>12</sup> Y. Yusa,<sup>47</sup> H. Yuta,<sup>1</sup> S. L. Zang,<sup>12</sup> C. C. Zhang,<sup>12</sup> J. Zhang,<sup>10</sup> L. M. Zhang,<sup>40</sup> Z. P. Zhang,<sup>40</sup> V. Zhilich,<sup>2</sup> T. Ziegler,<sup>37</sup> D. Žontar,<sup>21,15</sup> and D. Zürcher<sup>20</sup>

(The Belle Collaboration)

(Belle Collaboration)

<sup>1</sup>*Aomori University, Aomori*

<sup>2</sup>*Budker Institute of Nuclear Physics, Novosibirsk*

<sup>3</sup>*Chiba University, Chiba*

<sup>4</sup>*Chonnam National University, Kwangju*

<sup>5</sup>*Chuo University, Tokyo*

<sup>6</sup>*University of Cincinnati, Cincinnati, Ohio 45221*

<sup>7</sup>*University of Frankfurt, Frankfurt*

<sup>8</sup>*Gyeongsang National University, Chinju*

<sup>9</sup>*University of Hawaii, Honolulu, Hawaii 96822*

<sup>10</sup>*High Energy Accelerator Research Organization (KEK), Tsukuba*

<sup>11</sup>*Hiroshima Institute of Technology, Hiroshima*

<sup>12</sup>*Institute of High Energy Physics,*

*Chinese Academy of Sciences, Beijing*

<sup>13</sup>*Institute of High Energy Physics, Vienna*

<sup>14</sup>*Institute for Theoretical and Experimental Physics, Moscow*

<sup>15</sup>*J. Stefan Institute, Ljubljana*

<sup>16</sup>*Kanagawa University, Yokohama*

<sup>17</sup>*Korea University, Seoul*

<sup>18</sup>*Kyoto University, Kyoto*

<sup>19</sup>*Kyungpook National University, Taegu*

<sup>20</sup>*Swiss Federal Institute of Technology of Lausanne, EPFL, Lausanne*

<sup>21</sup>*University of Ljubljana, Ljubljana*

<sup>22</sup>*University of Maribor, Maribor*

<sup>23</sup>*University of Melbourne, Victoria*

<sup>24</sup>*Nagoya University, Nagoya*

<sup>25</sup>*Nara Women's University, Nara*

<sup>26</sup>*National Central University, Chung-li*

<sup>27</sup>*National Kaohsiung Normal University, Kaohsiung*

<sup>28</sup>*National United University, Miao Li*

<sup>29</sup>*Department of Physics, National Taiwan University, Taipei*

<sup>30</sup>*H. Niewodniczanski Institute of Nuclear Physics, Krakow*

<sup>31</sup>*Nihon Dental College, Niigata*

<sup>32</sup>*Niigata University, Niigata*

<sup>33</sup>*Osaka City University, Osaka*

<sup>34</sup>*Osaka University, Osaka*

<sup>35</sup>*Panjab University, Chandigarh*

<sup>36</sup>*Peking University, Beijing*

<sup>37</sup>*Princeton University, Princeton, New Jersey 08545*

<sup>38</sup>*RIKEN BNL Research Center, Upton, New York 11973*

<sup>39</sup>*Saga University, Saga*

<sup>40</sup>*University of Science and Technology of China, Hefei*

<sup>41</sup>*Seoul National University, Seoul*

<sup>42</sup>*Sungkyunkwan University, Suwon*

<sup>43</sup>*University of Sydney, Sydney NSW*

<sup>44</sup>*Tata Institute of Fundamental Research, Bombay*

<sup>45</sup>*Toho University, Funabashi*

<sup>46</sup>*Tohoku Gakuin University, Tagajo*

<sup>47</sup>*Tohoku University, Sendai*

<sup>48</sup>*Department of Physics, University of Tokyo, Tokyo*

<sup>49</sup>*Tokyo Institute of Technology, Tokyo*

<sup>50</sup>*Tokyo Metropolitan University, Tokyo*

<sup>51</sup>*Tokyo University of Agriculture and Technology, Tokyo*

<sup>52</sup>*Toyama National College of Maritime Technology, Toyama*

<sup>53</sup>*University of Tsukuba, Tsukuba*

<sup>54</sup>*Utkal University, Bhubaneswar*

<sup>55</sup>*Virginia Polytechnic Institute and State University, Blacksburg, Virginia 24061*

<sup>56</sup>*Yonsei University, Seoul*

## Abstract

We have searched for mixing in the  $D^0$ - $\overline{D}^0$  system by measuring the decay-time distribution of  $D^0 \rightarrow K^+ \pi^-$  decays. The analysis is based on  $90 \text{ fb}^{-1}$  of data collected at or near the  $\Upsilon(4S)$  resonance by the Belle detector operating at the KEKB asymmetric  $e^+ e^-$  collider. We fit the decay-time distribution for the mixing parameters  $x'$  and  $y'$  and also for the parameter  $R_D$ , which is the ratio of the doubly-Cabibbo-suppressed rate for  $D^0 \rightarrow K^+ \pi^-$  to the Cabibbo-favored rate for  $D^0 \rightarrow K^- \pi^+$ . We do these fits both assuming  $CP$  conservation and allowing for  $CP$  violation. We apply a frequentist method to the fit results to obtain a 95% C.L. region in the  $x'^2$ - $y'$  plane. This region is substantially more restrictive than previously-published results.

PACS numbers: 12.15.Ff, 13.25.Ft, 11.30.Er

The phenomenon of mixing among quark flavors has been observed in the  $K^0$ - $\overline{K}^0$  and  $B^0$ - $\overline{B}^0$  systems but not yet in the  $D^0$ - $\overline{D}^0$  system. The expected rate for  $D^0$ - $\overline{D}^0$  mixing within the Standard Model (SM) is small, well below current experimental upper limits [1]. Observation of mixing significantly larger than this prediction could indicate new physics. The short-distance contribution to mixing proceeds via the “box diagram,” which contains an internal loop and is thus sensitive to new particles and/or interactions. Such nonstandard processes may also give rise to  $CP$ -violating effects.

In this paper we present a search for  $D^0$ - $\overline{D}^0$  mixing and also  $CP$  violation ( $CPV$ ) in mixing with greater sensitivity than that of previous searches. The data sample consists of  $90\text{ fb}^{-1}$  recorded by the Belle experiment running at the KEKB asymmetric  $e^+e^-$  collider [2]. The Belle detector [3] consists of a three-layer silicon vertex detector (SVD), a 50-layer central drift chamber (CDC), an array of aerogel threshold Cherenkov counters (ACC), time-of-flight scintillation counters (TOF), and an electromagnetic calorimeter comprised of CsI(Tl) crystals. These detectors are located within a superconducting solenoid coil providing a 1.5 T magnetic field. An iron flux-return located outside the coil is instrumented to identify muons and detect  $K_L^0$  mesons.

The dominant two-body decay of the  $D^0$  is the Cabibbo-favored (CF) decay  $D^0 \rightarrow K^-\pi^+$  [4]. We search for mixing by reconstructing the “wrong-sign” decay  $D^0 \rightarrow K^+\pi^-$ , which would arise from a  $D^0$  mixing to  $\overline{D}^0$  and subsequently decaying via  $\overline{D}^0 \rightarrow K^+\pi^-$ . The flavor of the  $D$  is identified by requiring that it originate from  $D^{*+} \rightarrow D^0\pi^+$  or  $D^{*-} \rightarrow \overline{D}^0\pi^-$  and noting the charge of the accompanying pion. In addition to arising via mixing,  $D^0 \rightarrow K^+\pi^-$  can also occur via a doubly-Cabibbo-suppressed (DCS) amplitude. This has a different decay-time dependence than that of mixing, and the two processes can be distinguished by measuring the decay-time distribution. This method has previously been used by FNAL E791 [5], CLEO [6], and BaBar [7] to constrain  $D^0$ - $\overline{D}^0$  mixing and measure or constrain the DCS decay rate.

The SM parameters used to characterize mixing are  $x \equiv \Delta m/\overline{\Gamma}$  and  $y \equiv \Delta\Gamma/(2\overline{\Gamma})$ , where  $\Delta m$  and  $\Delta\Gamma$  are the differences in mass and decay width between the two  $D^0$ - $\overline{D}^0$  mass eigenstates, and  $\overline{\Gamma}$  is the mean decay width. For  $|x|, |y| \ll 1$  and negligible  $CPV$ , the decay time distribution for  $D^0 \rightarrow K^+\pi^-$  can be expressed as:

$$\frac{dN}{dt} \propto e^{-\overline{\Gamma}t} \left[ R_D + \sqrt{R_D} y'(\overline{\Gamma}t) + \frac{x'^2 + y'^2}{4} (\overline{\Gamma}t)^2 \right], \quad (1)$$

where  $R_D$  is the ratio of DCS to CF decay rates,  $x' = x \cos \delta + y \sin \delta$ ,  $y' = y \cos \delta - x \sin \delta$ , and  $\delta$  is the strong phase difference between DCS and CF amplitudes. The first term in brackets is due to the DCS amplitude, the last term is due to mixing, and the middle term is due to interference between the two processes. The time-integrated rate for  $D^0 \rightarrow K^+\pi^-$  decays relative to CF decays is  $R_D + \sqrt{R_D} y' + (x'^2 + y'^2)/2$ .

To allow for  $CP$  violation, we follow [7] and apply Eq. (1) to  $D^0$  and  $\overline{D}^0$  decays separately. This results in six observables:  $\{R_D^+, x'^{+2}, y'^+\}$  for  $D^0$  and  $\{R_D^-, x'^{-2}, y'^-\}$  for  $\overline{D}^0$ .  $CP$  violation can then be parametrized by the asymmetries  $A_D = (R_D^+ - R_D^-)/(R_D^+ + R_D^-)$  and  $A_M = (R_M^+ - R_M^-)/(R_M^+ + R_M^-)$ , where  $R_M^\pm = 0.5 \times (x'^{\pm 2} + y'^{\pm 2})$ . The asymmetry  $A_D$  characterizes  $CPV$  in the DCS decay amplitude, and the asymmetry  $A_M$  characterizes  $CPV$  in  $D^0$ - $\overline{D}^0$  mixing. The observables are related to  $x'$  and  $y'$  via:

$$x'^\pm = \left[ \frac{1 \pm A_M}{1 \mp A_M} \right]^{\frac{1}{4}} (x' \cos \phi \pm y' \sin \phi) \quad (2)$$

$$y'^{\pm} = \left[ \frac{1 \pm A_M}{1 \mp A_M} \right]^{\frac{1}{4}} (y' \cos \phi \mp x' \sin \phi) , \quad (3)$$

where  $\phi$  is a weak phase and characterizes *CPV* occurring via interference between mixed and unmixed decay amplitudes. Note that  $x'^{\pm}$ ,  $y'^{\pm}$  are unchanged by the transformation  $x' \rightarrow -x'$ ,  $y' \rightarrow -y'$ , and  $\phi \rightarrow \phi + \pi$ ; thus for definiteness we restrict  $\phi$  to the range  $|\phi| < \pi/2$ .

We select  $D^0 \rightarrow K^-\pi^+$  decays by requiring two oppositely-charged tracks with at least four SVD hits ( $\geq 2$  in both  $r\phi$  and  $z$  views) that satisfy  $K$  and  $\pi$  identification criteria. These criteria are  $\mathcal{L}_K > 0.6$  and  $\mathcal{L}_\pi > 0.4$ , where  $\mathcal{L}$  is the relative likelihood for a track to be a  $K$  or  $\pi$  based on  $dE/dx$  information in the CDC and the responses of the TOF and ACC systems. These likelihood criteria have efficiencies of 88.0% and 88.5%, respectively, with corresponding  $\pi/K$  misidentification rates of 8.5% and 8.8%. We subsequently combine the  $D^0$  candidate with an additional low-momentum pion ( $\pi_{\text{slow}}$ ) to form a  $D^{*+} \rightarrow D^0\pi^+$  candidate. Candidates in which the charge of  $\pi_{\text{slow}}$  is opposite (equal to) that of the  $K^\pm$  are referred to as “right-sign” or RS (“wrong-sign” or WS) decays. To reject WS background from  $D^0 \rightarrow K^-\pi^+$  in which the  $K$  is misidentified as  $\pi$  and the  $\pi$  is misidentified as  $K$ , we reject events in which  $|m_{K\pi(\text{swapped})} - m_{D^0}| < 28 \text{ MeV}/c^2$ . To reject WS background from  $D^0 \rightarrow K^+K^-$  and  $D^0 \rightarrow \pi^+\pi^-$ , we require  $1.81 \text{ GeV}/c^2 < m_{K\pi} < 1.91 \text{ GeV}/c^2$ . Finally, to eliminate  $D^*$ ’s originating from  $B$  decays, we require  $p_{D^*}^{\text{cm}} > 2.5 \text{ GeV}/c$ .

The  $D^0$  vertex position is obtained by fitting the daughter  $K/\pi$  tracks. The  $D^*$  vertex position is taken as the intersection of the  $D^0$  momentum vector with the interaction profile (IP) region. We require a good  $\chi^2$  for each vertex fit. The IP region is calculated every 10000 hadronic interactions from the distribution of primary vertices and has a vertical dimension of only  $\sim 5 \mu\text{m}$ . The momentum of  $\pi_{\text{slow}}$  is refitted with the constraint that it originates from the  $D^*$  vertex. The  $D^0$  decay time is calculated as  $(\ell_{D^0}/p_{D^0}) \times m_{D^0}$ , where  $\ell_{D^0}$  is the distance between the  $D^0$  and  $D^*$  vertices projected onto the  $\vec{p}_{D^0}$  direction. The decay-time resolution is typically 0.2 ps.

We measure the parameters  $R_D$ ,  $x'^2$  and  $y'$  of Eq. (1) via an unbinned maximum likelihood fit to the WS decay-time distribution. The likelihood function consists of probability density functions (pdf’s) for signal and several types of background. These pdf’s depend on the decay time, the  $D^0$  candidate mass  $m_{K\pi}$ , and the kinetic energy released  $Q \equiv m_{K\pi\pi_{\text{slow}}} - m_{K\pi} - m_\pi$ . The latter equals only  $5.85 \text{ MeV}/c^2$  for  $D^{*+} \rightarrow D^0\pi_{\text{slow}}^+ \rightarrow K\pi\pi_{\text{slow}}^+$  decays, which is close to threshold.

The signal pdf for event  $i$  is smeared by a resolution function

$$R_i = (1 - f_{\text{tail}}) G(t_i - t', \sigma_{t,i} ; \mu, S) + f_{\text{tail}} G(t_i - t', \sigma_{t,i} ; \mu, S_{\text{tail}}) , \quad (4)$$

where the  $G$ ’s are Gaussians with common mean  $\mu$  and standard deviations  $(S \times \sigma_{t,i})$  and  $(S_{\text{tail}} \times \sigma_{t,i})$ , and  $\sigma_{t,i}$  is the uncertainty in decay time  $t$  for event  $i$ . The parameters  $f_{\text{tail}}$ ,  $\mu$ , and scaling factors  $S$  and  $S_{\text{tail}}$  are determined from data. The background pdf’s are smeared by similar resolution functions, as described below. To check the resolution function, we fit the RS sample in the same manner as the WS sample except that the signal pdf has a purely exponential time dependence.

There are four significant backgrounds to the WS sample: (a) random  $\pi$  background, in which a random  $\pi^+$  is paired with a true  $\overline{D}^0 \rightarrow K^+\pi^-$  decay (the pdf is peaked in  $m_{K\pi}$  but broad in  $Q$ ); (b)  $D^{*+} \rightarrow D^0\pi^+$  followed by  $D^0$  decaying to  $\geq 3$ -body final states (the pdf is broad in  $m_{K\pi}$  and broad but enhanced in  $Q$ ); (c)  $D^+/D_s^+$  decays; and (d) combinatorial

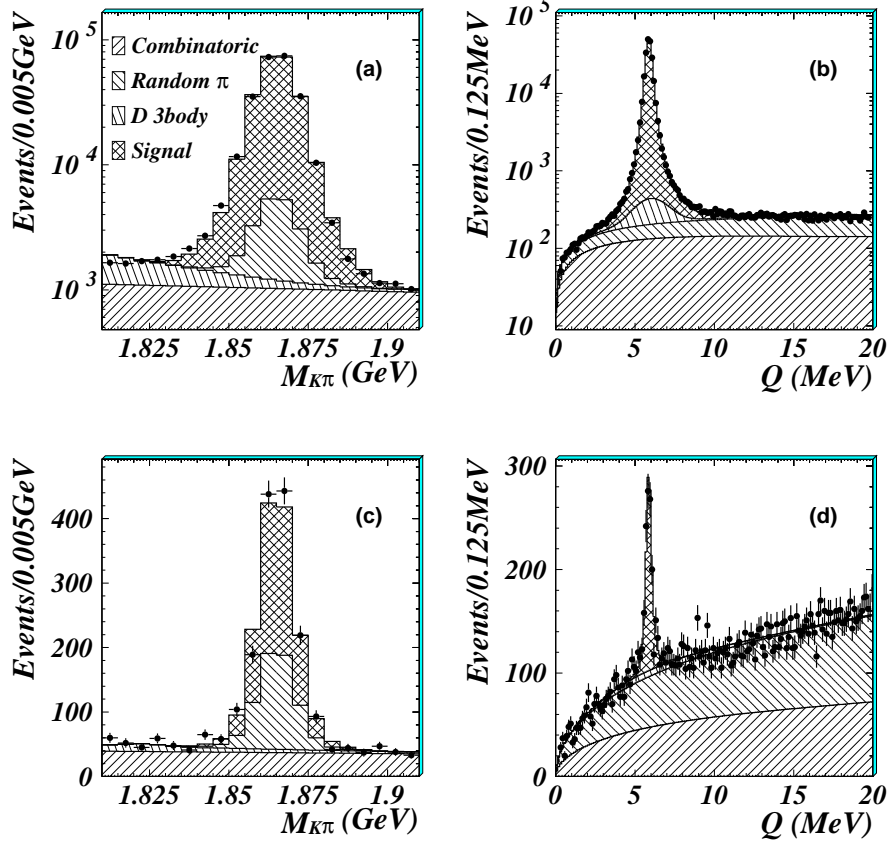


FIG. 1: Distributions of (a) RS  $m_{K\pi}$  with  $0 < Q < 20$  MeV; (b) RS  $Q$  with  $1.81 \text{ GeV}/c^2 < m_{K\pi} < 1.91 \text{ GeV}/c^2$ ; (c) WS  $m_{K\pi}$  with  $|Q - 5.9 \text{ MeV}| < 0.6 \text{ MeV}$ ; and (d) WS  $Q$  with  $|m_{K\pi} - m_{D^0}| < 20 \text{ MeV}/c^2$ . Superimposed on the data (points with error bars) are projections of the  $m_{K\pi}$ - $Q$  fit.

background. These backgrounds have different decay-time distributions. We determine the level of each background by performing a two-dimensional fit to the  $m_{K\pi}$ - $Q$  distribution. When fitting the RS sample, the  $m_{K\pi}$  and  $Q$  means and widths for signal are floated; when fitting the WS sample, these means and widths are fixed to the values obtained from the RS fit. Also for the WS fit, the relative normalization between  $D^+/D_s^+$  and  $\geq 3$ -body backgrounds is fixed to the value obtained from Monte Carlo (MC) simulation. The RS fit finds  $227721 \pm 497$   $D^0 \rightarrow K^-\pi^+$  decays, and the WS fit finds  $845 \pm 40$   $D^0 \rightarrow K^+\pi^-$  decays. The ratio  $R_{WS} \equiv \Gamma(D^0 \rightarrow K^+\pi^-)/\Gamma(D^0 \rightarrow K^-\pi^+) = (0.371 \pm 0.018)\%$  (statistical errors only). The ratio of WS signal to background is 0.9; the latter is mostly random  $\pi$  (59%) and combinatorial (36%). The  $m_{K\pi}$  and  $Q$  distributions are shown in Fig. 1 along with projections of the fit result. These projections agree well with the data.

To fit the decay-time distributions of RS and WS samples, we consider the  $4\sigma$  region  $|m_{K\pi} - m_{D^0}| < 22 \text{ MeV}/c^2$  and  $|Q - 5.9 \text{ MeV}| < 1.5 \text{ MeV}/c^2$ . The signal and background yields (which multiply the respective pdf's in the likelihood function) are determined via the  $m_{K\pi}$ - $Q$  fit described above; the resulting value of  $R_{WS}$  constrains the decay-time fit normalization. The decay-time distributions for the backgrounds before smearing are taken to be:  $e^{-t/\tau_{D^0}}$  for random  $\pi$  background,  $e^{-t/\tau_{D3b}}$  for  $\geq 3$ -body  $D^0$  background,  $e^{-t/\tau_{Dch}}$  for  $D^+/D_s^+$  background, and  $\delta(t)$  for combinatorial background. The parameter  $\tau_{D3b}$  is

obtained from fitting sideband data, and  $\tau_{Dch}$  is obtained from MC simulation. These time distributions are convolved with resolution functions. For random- $\pi$  background (and the small multi-body  $D^0/D^+/D_s^+$  background), the resolution function used is the same as that for signal; for combinatorial background, the resolution function used has the same form but the parameters ( $f_{tail}^{(comb)}$ ,  $S^{(comb)}$ ,  $S_{tail}^{(comb)}$ ) are determined from fitting sideband data.

The fitting procedure is implemented in steps as follows. We first fit the RS signal region using a simple background model to obtain a first estimate of signal resolution function parameters. We use this resolution function to fit an RS sideband region, which yields  $f_{tail}^{(comb)}$ ,  $S^{(comb)}$ ,  $S_{tail}^{(comb)}$ , and  $\tau_{D3b}$  for RS background. We then fit the RS signal region with these parameters fixed, which yields  $\mu$ ,  $f_{tail}$ ,  $S$ ,  $S_{tail}$  and, as a check,  $\tau_{D^0}$ . We subsequently use this resolution function to fit the WS sideband region, obtaining  $f_{tail}^{(comb)}$ ,  $S^{(comb)}$ ,  $S_{tail}^{(comb)}$ , and  $\tau_{D3b}$  for WS background. Finally, we fit the WS signal region, fixing these background parameters and those of the signal resolution function; this yields  $R_D$ ,  $x'^2$ , and  $y'$ .

The above fitting procedure has undergone several checks. In MC simulation, background parameters obtained from the sideband region fit describe well the background in the signal region. The resolution function obtained from data is very similar to that obtained from the MC. The lifetime  $\tau_{D^0}$  obtained from the RS signal region fit is  $415.1 \pm 1.4$  ps, consistent with the PDG value [9]; the  $\chi^2$  of the fit projection is 56.0 for 55 bins. We have generated MC samples of the same size as that of the data sample, adding the corresponding amount of background, and repeated the fitting procedure. For nine sets of  $(x'^2, y')$  values (spanning the ranges  $[0, 2] \times 10^{-3}$  and  $[-2, 2] \times 10^{-2}$ , respectively), the fit recovers values consistent with the generated values. For these nine sets we have also generated ensembles of “toy” MC experiments, i.e., without detector simulation, smearing the time distributions and adding the appropriate amount of background. Fitting these experiments shows negligible fit bias, and the  $x'^2, y'$  values obtained are in all cases consistent with the generated values.

Thus far, all cut optimization and tests of the fitting procedure were done in a “blind” manner, i.e., without fitting events in the WS signal region. We now fix all cuts and fit this sample. Four separate fits are done, yielding the results listed in Table I; the errors listed are MINOS errors [8]. For the first fit we require that  $CP$  be conserved; the projection of this fit superimposed on the data is shown in Fig. 2. The central value obtained for  $x'^2$  is negative (i.e., outside the physical region); thus the most-likely value for  $x'$  is zero, and we subsequently refit the data fixing  $x'^2 = 0$ . The  $\chi^2$  of this fit projection is 73.2 for 60 bins, which is satisfactory. The  $y'$  value obtained is  $\sim 2\sigma$  from zero; when we generate MC experiments with this value (and  $x'^2 = 0$ ), we find that the probability of obtaining an  $x'^2$  value as negative as what we measure in the data is 8%. For the third fit we consider the case of no mixing and set  $x'^2 = y' = 0$ ; the  $\chi^2$  of this fit projection is 75.6 for 60 bins, somewhat worse than for the case of mixing. Finally, for the last fit we relax the assumption of  $CP$ -invariance and fit the  $D^0 \rightarrow K^+\pi^-$  and  $\bar{D}^0 \rightarrow K^-\pi^+$  samples separately; this yields  $\{R_D^+, x'^{+2}, y'^+\}$  and  $\{R_D^-, x'^{-2}, y'^-\}$ . We calculate  $A_D$  and  $A_M$  and insert these values into Eqs. (2) and (3) to solve for  $x'^2, y'$ , and the  $CPV$  parameter  $\phi$ .

To obtain 95% CL limits on  $x'^2$  and  $y'$ , we use a frequentist method with Feldman-Cousins ordering [10] similar to that used in Ref. [7]. For points  $\vec{\alpha} = (x'^2, y')$ , we generate ensembles of toy MC experiments and fit them using the same procedure as that used for the data. For each experiment we record the difference in likelihood  $\Delta L = \ln L_{\max} - \ln L(\vec{\alpha})$ ; the locus of points  $\vec{\alpha}$  for which 95% of the ensemble has  $\Delta L$  less than that of the data sample is taken as the 95% CL contour. This contour is shown in Fig. 3.

To allow for  $CPV$ , we obtain separate  $1 - \sqrt{0.05} = 77.6\%$  CL contours for  $(x'^{+2}, y'^+)$  and

TABLE I: Summary of results from the separate likelihood fits. The 95% CL intervals are obtained from a frequentist method (see text) and include systematic errors.

Fit Case	Parameter	Fit Result ( $\times 10^{-3}$ )	95% CL interval ( $\times 10^{-3}$ )
No <i>CPV</i>	$x'^2$	$-1.53^{+0.80}_{-1.00}$	$x'^2 < 0.81$
	$y'$	$25.4^{+11.1}_{-10.2}$	$-8.2 < y' < 16$
	$R_D$	$2.87 \pm 0.37$	$2.7 < R_D < 4.0$
No <i>CPV</i>	$y'$	$6.0 \pm 3.3$	—
$x' = 0$ (fixed)	$R_D$	$3.43 \pm 0.26$	—
No mixing	$R_D$	$3.81 \pm 0.17$	—
<i>CPV</i> allowed	$A_D$	$-80 \pm 77$	$-250 < A_D < 110$
	$A_M$	$987^{+13}_{-487}$	$-991 < A_M < 1000$
	$x'^2$	—	$x'^2 < 0.89$
	$y'$	—	$-30 < y' < 27$

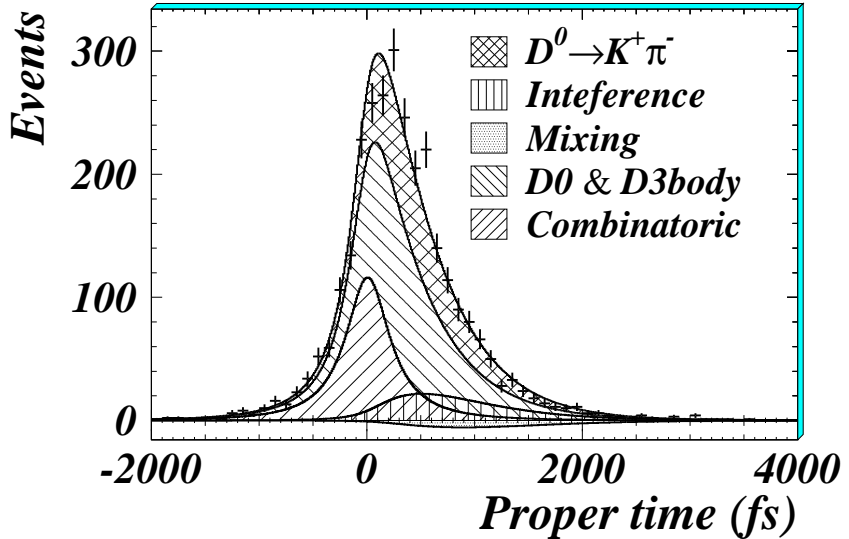


FIG. 2: The decay-time distribution for WS events satisfying  $|m_{K\pi} - m_{D^0}| < 22$  MeV/ $c^2$  and  $|Q - 5.9$  MeV| < 1.5 MeV/ $c^2$ . Superimposed on the data (plotted as points with error bars) are projections of the decay-time fit.

$(x'^{-2}, y'^{-})$ . We then combine points on the  $(x'^{+2}, y'^{+})$  contour with points on the  $(x'^{-2}, y'^{-})$  contour and use these sets of values to solve Eqs. (2) and (3) for  $x'^2$  and  $y'$ . Because the relative sign of  $x'^{+}$  and  $x'^{-}$  is unknown, there are two possible solutions, one for each relative sign. We plot both solutions in the  $(x'^2, y')$  plane and take the outermost envelope of points to be the 95% CL contour allowing for *CPV*. This contour has an irregular shape due to the two solutions. Because the contour includes the point  $x'^2 = y' = 0$ , we cannot constrain  $\phi$  at this confidence level.

We evaluate systematic errors by varying parameters used to select and fit the data within their uncertainties and recording the new values  $\vec{\alpha}_{\text{new}}$  obtained from the fit. These values

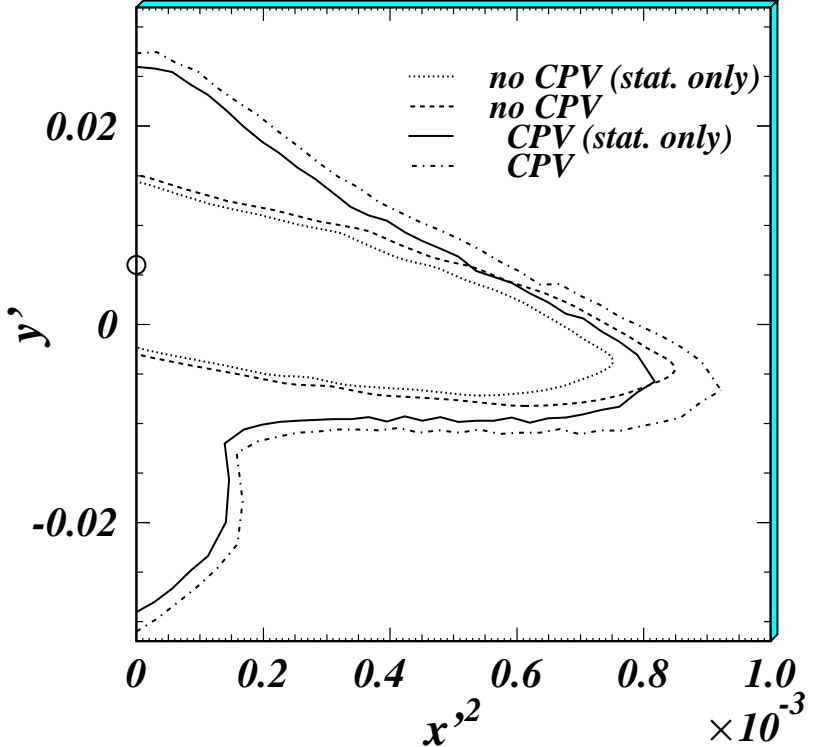


FIG. 3: 95% CL regions for  $(x'^2, y')$ . The dotted (dashed) contour is statistical (statistical and systematic) and corresponds to the case of  $CP$  conservation. The solid (dashed-dotted) contour is statistical (statistical and systematic) and corresponds to the case where  $CPV$  is allowed. The open circle represents the most-likely value when  $CP$  is conserved and  $x'^2$  is constrained to be  $\geq 0$ .

are shifted with respect to the original central value  $\vec{\alpha}_0$ . We find the significance  $m$  of a shift by taking the difference of log likelihoods and dividing by 2.30 (corresponding to 68.3% confidence in two dimensions):  $m^2 = -2[\ln L(\vec{\alpha}_{\text{new}}) - \ln L(\vec{\alpha}_0)]/2.30$ . We add in quadrature the significances of all individual shifts to obtain an overall scaling factor  $\sqrt{1 + \sum m_i^2}$ . We scale the 95% CL statistical contour by this factor to include systematic errors. As a check, we generate an ensemble of toy MC experiments with  $\vec{\alpha}_{MC} = (0., 0.006)$  and fit them to confirm that 68.3% of the ensemble satisfies  $-2[\ln L(\vec{\xi}) - \ln L(\vec{\alpha}_{MC})] < 2.3$ , where  $\vec{\xi}$  is the central value for an experiment.

The parameters varied include kaon and pion identification criteria, the  $\chi^2$  of the vertex fit, background shape and normalization parameters, and resolution function parameters for both signal and combinatorial background. The largest shift in  $(x'^2, y')$  occurs for the  $D^{*+}$  momentum cut; when this is varied over a significant range,  $(\Delta x'^2/x'^2)_{\text{max}} = 12\%$ ,  $(\Delta y'/y')_{\text{max}} = 10\%$ , and  $\Delta(-2 \ln L) = 0.092$ . The overall scaling factor is  $\sqrt{1 + \sum m_i^2} = 1.08$ . For the general case allowing for  $CPV$ , we scale the  $D^0$  and  $\bar{D}^0$  contours separately before combining. The rescaled 95% CL contours (now including systematic errors) are shown in Fig. 3: the dashed contour corresponds to the  $CP$ -conserving case and the dash-dotted contour to the general case. Projecting these contours onto the coordinate axes gives the 95% CL intervals for  $x'^2$  and  $y'$  listed in Table I.

In summary, we have searched for mixing and  $CP$  violation in the  $D^0$ - $\bar{D}^0$  system using WS  $D^0 \rightarrow K^+ \pi^-$  decays. In  $90 \text{ fb}^{-1}$  of data we find no significant evidence for these processes

and set limits on the mixing parameters  $x'^2$  and  $y'$  and the  $CP$  asymmetry parameters  $A_D$  and  $A_M$ . The limits for  $x'^2$  and  $y'$  are more stringent than previously published results.

We thank the KEKB group for the excellent operation of the accelerator, the KEK Cryogenics group for the efficient operation of the solenoid, and the KEK computer group and the National Institute of Informatics for valuable computing and Super-SINET network support. We acknowledge support from the Ministry of Education, Culture, Sports, Science, and Technology of Japan and the Japan Society for the Promotion of Science; the Australian Research Council and the Australian Department of Education, Science and Training; the National Science Foundation of China under contract No. 10175071; the Department of Science and Technology of India; the BK21 program of the Ministry of Education of Korea and the CHEP SRC program of the Korea Science and Engineering Foundation; the Polish State Committee for Scientific Research under contract No. 2P03B 01324; the Ministry of Science and Technology of the Russian Federation; the Ministry of Education, Science and Sport of the Republic of Slovenia; the National Science Council and the Ministry of Education of Taiwan; and the U.S. Department of Energy.

---

\* on leave from Nova Gorica Polytechnic, Nova Gorica

- [1] For a comprehensive review see: S. Bianco, F. L. Fabbri, D. Benson, and I. Bigi, Riv. Nuovo Cim. **26N7-8**, 1 (2003).
- [2] S. Kurokawa and E. Kikutani, Nucl. Instr. Meth. A **499**, 1 (2003).
- [3] A. Abashian *et al.* (Belle), Nucl. Instr. Meth. A **479**, 117 (2002).
- [4] Charge-conjugate modes are included throughout this paper unless noted otherwise.
- [5] E. Aitala *et al.* (E791), Phys. Rev. D **57**, 13 (1998).
- [6] R. Godang *et al.* (CLEO), Phys. Rev. Lett. **84**, 5038 (2000).
- [7] B. Aubert *et al.* (BaBar), Phys. Rev. Lett. **91**, 171801 (2003).
- [8] <http://wwwasdoc.web.cern.ch/wwwasdoc/minuit/node7.html>
- [9] S. Eidelman *et al.*, Phys. Lett. B **592**, 1 (2004).
- [10] G. J. Feldman and R. D. Cousins, Phys. Rev. **D57**, 3873 (1998).